NMR Studies and Conformational Analysis of a DNA Four-Way Junction Formed in a Linear Synthetic Oligonucleotide†

Jeroen A. Pikkemaat, Hans van den Elst, Jacques H. van Boom, and Cornelis Altona*

Leiden Institute of Chemistry, Gorlaeus Laboratories, P.O. Box 9502, NL-2300 RA Leiden, The Netherlands

Received July 27, 1994; Revised Manuscript Received September 26, 1994®

ABSTRACT: A linear DNA oligomer (M_r 14 000, 46 nucleotides) was especially designed, chemically synthesized, and studied by means of ^{1}H NMR spectroscopy. The design of the oligomer was guided by the idea that incorporation of three short palindromic sequences, each interspersed by 5′-CTTG-3′ motifs at predetermined positions in the oligomer, would give rise to the formation of three stable minihairpin loops [Ippel, J. H., et al. (1992) *J. Biomol. Struct. Dyn. 9*, 1−16], which in turn were expected to encourage further folding of the strand into a stable four-way junction containing three "hairpin" arms and an open-ended duplex stem as the fourth arm. Linear DNA four-way junctions constructed according to this concept can be more compact and are therefore expected to be more suitable as model compounds for conformational studies compared to junctions that are built from two or more separate strands. A stable cruciform conformation was substantiated for the 46-mer in aqueous solution in the presence of Mg^{2+}. Complete sequential ^{1}H NMR assignments of the nonexchangeable protons (except H4′, H5′, and H5″) were obtained with the aid of NOESY and HOHAHA experiments. The NMR data gave evidence for the expected existence of minihairpin-loop structures at the three 5′-CTTG-3′ motifs in the sequence. The complementary stem domains adopt a regular B-DNA form. Watson−Crick type base pairing is preserved for all residues in the stem domains, including the residues at the center of the junction. A systematic investigation of the interresidual NOEs observed between the protons of the eight central residues revealed the complete stacking pattern of the residues at the branch point.

The principle of two different DNA duplexes forming a single, branched structure was originally proposed by Holliday (1964) on purely theoretical grounds. Such branched DNA junctions, known as Holliday junctions, are supposed to be the central intermediate in DNA-recombination processes (Holliday, 1964; Meselson & Radding, 1975; Orr-Weaver et al., 1981). The secondary structure at the center of a Holliday junction is formally equivalent to the four-way branch point (junction) at the center of cruciform structures which may be induced at inverted-repeat sequences in a DNA duplex (Platt, 1955; Gierer, 1966; Hseih & Wang, 1975). Since the publication of experimental evidence for the actual existence of transient cruciform structures at inverted-repeat sequences in negatively supercoiled DNA (Gellert et al., 1979; Lilley, 1980; Panayotatos & Wells, 1981) and the discovery of Holliday-junction resolving proteins (Mizuuchi et al., 1982; De Massey et al., 1984; Hsu & Landy, 1984; Symington & Kolodner, 1985), the importance of the four-way junction as a general DNA folding principle is now widely accepted. In-depth knowledge of its conformation and thermodynamics could well be the key to a better understanding of the process of DNA recombination. Several global features of the conformation of four-way junctions have been revealed by various, mainly biochemical, methods. These are reviewed by Duckett et al. (1992) and Lilley and Clegg (1993). An experiment-based three-dimensional structure of a four-way junction on the "atomic level", however, has not yet been reported.

Four-way junctions in inverted-repeat sequences are intrinsically difficult to study because of spontaneous branch migration (Thompson et al., 1976). For this reason immobilized model compounds were constructed artificially by hybridizing four DNA strands with tailored sequences (Bell & Byers, 1979; Seeman, 1982; Seeman & Kallenbach, 1983). Even so, progress has been slow. In contrast to other structural motifs in DNA like B-DNA, A-DNA, Z-DNA, hairpin loops, and triple- and quadruple helices, it appears to be very difficult to crystallize a four-way junction for X-ray studies or to construct a suitable model compound which is both stable and sufficiently compact for detailed conformational analysis using NMR[1] techniques. The smallest stable four-way junction reported so far in the literature is an immobilized synthetic junction which is composed of four different, specially designed, oligonucleotides in a 1:1:1:1 ratio (Kallenbach et al., 1983). Each oligonucleotide contains 16 nucleotides which together yield a compound DNA structure of 64 residues. In spite of the still considerable number of residues, this compound enabled the first NMR study of a four-way junction (Wemmer et al., 1985). A comparison of the imino-proton spectra of the individual

† This research was supported by the Netherlands Foundation for Chemical Research (SON) with financial aid from the Netherlands Organization for Scientific Research (NWO).

* To whom correspondence should be addressed.

® Abstract published in *Advance ACS Abstracts,* November 1, 1994.

[1] Abbreviations: NMR, nuclear magnetic resonance; 2D, two dimensional; NOE, nuclear Overhauser enhancement; NOESY, 2D NOE and exchange spectroscopy; FPLC, fast protein liquid chromatography; TEAB, triethylammonium bicarbonate; EDTA, ethylenediaminetetraacetic acid, disodium salt; TMA, tetramethylammonium chloride (Me_4HCl); DSS, 3-(trimethylsilyl)-1-propanesulfonic acid, sodium salt; HOHAHA, homonuclear Hartmann−Hahn; ppm, parts per million.

0006-2960/94/0433-14896$04.50/0

Scheme 1. Schematic Structures and Base Sequences of the Four-Way Junction, J4, and the Previously Studied Double-Hairpin Structure, DB16[a]

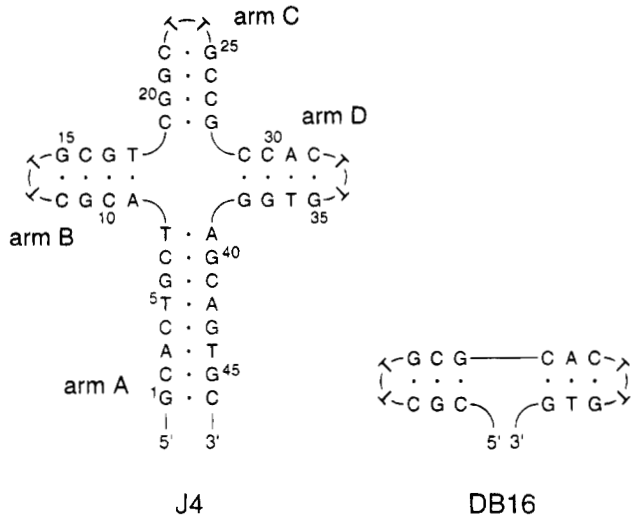

[a] Note the similarities between the base sequences of arms B and D in J4 and those of the arms in DB16.

duplex arms with the imino-proton spectrum of the intact four-stranded junction suggested that base pairing occurs at the branch point. Unfortunately, the resonance assignment of such large DNA compounds is extremely difficult, due to severe spectral overlap. Nevertheless, Chen et al. (1991, 1993) recently reported an advanced assignment of Kallenbach's compound and of a highly related four-way junction. NOEs[1] collected by Chen et al. for the exchangeable protons of the residues directly adjacent to the branch point, though relatively few in number, were consistent with a coaxially stacked conformation. The reported NOEs for the nonexchangeable protons at the branch point were less consistent due to the complexity of the NOESY[1] spectra. For a proper structure determination more accurate distance constraints are necessary.

On the basis of our accumulated knowledge concerning the thermodynamic stability and conformational properties of small hairpin loops in DNA, we expect that the number of residues required to construct stable four-way junctions can be significantly reduced if highly stable H2-type minihairpin loops (Pieters et al., 1990; Ippel et al., 1992) are incorporated in the arms of the molecule. In this report we show that a linear DNA fragment consisting of 46 residues (henceforth called J4) yields a stable four-way junction in the presence of Mg^{2+} ions. As shown in Scheme 1, the base sequence of J4 is based upon a previously studied double-hairpin structure DB16 (J. A. Pikkemaat and C. Altona, unpublished results). The analogy with this smaller fragment and the characteristic NMR pattern of the three 5′-CTTG-3′ hairpin-loop motifs enabled a fast and straightforward sequential assignment of the nonexchangeable protons using relatively simple NMR techniques. NOE data indicate that the major part of the molecule adopts a B-DNA type duplex conformation, except for the three hairpin-loop motifs which adopt H2-type minihairpin-loop conformations, and four out of the eight central residues directly adjacent to the four-way branch point. For these central residues a significant number of highly unusual long-range NOEs were observed, which imply a fully stacked conformation as was postulated by Cooper and Hagerman (1987).

MATERIALS AND METHODS

DNA Synthesis. Oligomer J4 was assembled on large scale (5 μmol) by solid-phase synthesis on a fully automated synthesizer (Gene Assembler, Pharmacia) using commercially available 2′-deoxynucleoside 3′-*O*-(2-cyanoethyl-*N*,*N*-diisopropyl)phosphoramidites. Controlled pore glass (CPG-AP, 200 mg), covalently linked to the appropriate nucleoside was used as solid support. After deprotection and cleavage from the polymer support by treatment (24 h) with aqueous NH_3 (25%) at 50 °C, the oligonucleotide was analyzed by FPLC[1] and purified on Sephadex G-50 (150 cm × 2 cm^2) using 0.05 M TEAB[1] buffer both as solvent and as eluens. The appropriate fractions were pooled, concentrated to a small volume, and coevaporated with aqueous NH_3 in order to remove excess TEAB. Elution through a column of Dowex 50W X4 cation-exchange resin (100−200 mesh, Na^+ form) finally yielded the Na^+ salt of the oligomer.

NMR Sample Preparation. The entire supply of the purified oligonucleotide was used for each NMR sample. Sample volumes were typically 450−500 μL, resulting in concentrations of ca. 1.4 mM oligomer. Initially a sample was prepared for measurements in D_2O in the absence of salt by lyophilizing the oligonucleotide twice from D_2O (99.72%) and finally dissolving in 450−500 μL D_2O (99.95%). Prior to lyophilization, a trace of EDTA[1] (0.1 mM) was added in order to neutralize the effects of paramagnetic impurities, TMA[1] was added as chemical-shift reference, and the pD values were adjusted with DCl to 7.0 (not corrected for isotope effects). A sample for measurements in D_2O in the presence of magnesium ions was prepared from the previous sample by the addition of a stock solution containing 5 mM $MgCl_2$ and 50 mM NaCl in D_2O (99.75%). After lyophilization, the sample was taken up again in ca. 500 μL of D_2O for analysis. For the observation of exchangeable protons a third sample with virtually the same salt concentration was made by lyophilizing the previous sample and dissolving again in ca. 500 μL of H_2O/D_2O (9:1, v/v). Slightly acidic conditions (pH 6.0) were chosen for the experiments in H_2O in order to suppress proton exchange with the solvent. In order to eliminate alternative (metastable) structures possibly formed during the sample preparation, all samples were heated to 65 °C and cooled down slowly to room temperature prior to the NMR experiments.

^1H and ^{31}P Chemical-Shift Reference. TMA was used as an internal chemical-shift reference for the ^1H NMR spectra. The TMA scale was converted to the more commonly used DSS[1] scale by adding 3.184 ppm to the measured chemical shift values (Hartel et al., 1982). ^{31}P NMR spectra were calibrated using 85% H_3PO_4 as external chemical-shift reference.

NMR Spectroscopy. 600-MHz ^1H NMR spectra were recorded on a Bruker AM600 spectrometer equipped with an Aspect 3000 computer, using the Bruker DISNMR88 software package. For the acquisition of one-dimensional 600-MHz ^1H NMR spectra typically ca. 200 transients were accumulated with 8192 complex data points and a spectral width of 5405 Hz. The residual HDO signal was suppressed by a weak irradiation at the HDO frequency during the preparation period (1.0 s). All homonuclear 2D NMR spectra were measured at 600 MHz in phase-sensitive mode, using time-proportional phase incrementation (TPPI) (Marion &

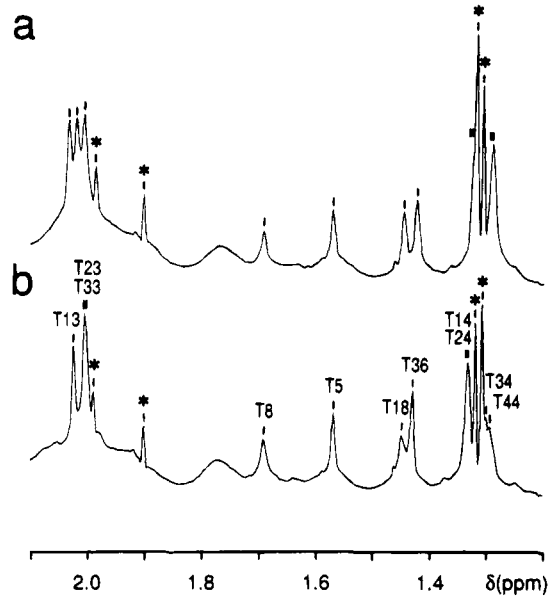

FIGURE 1: Methyl-proton region of the one-dimensional 600-MHz ^{1}H NMR spectrum of J4 in D_2O (5 mM $MgCl_2$; 50 mM NaCl) at two different temperatures, (a) 287 K and (b) 302 K. Signals caused by impurities are indicated with an asterisk (*).

Wüthrich, 1983). Unless stated differently, the 2D experiments were acquired with 80 scans, a spectral width of 5405 Hz in both domains, 2K complex data points in the t_2 domain, and 400 t_1 increments. Suppression of the HDO signal was achieved by the method described above. Two NOESY spectra (Jeener et al., 1979; Macura & Ernst, 1980; Macura et al., 1981) in D_2O were recorded at 302 K with two different mixing times, 75 and 350 ms. A HOHAHA[1] experiment (32 scans, 512 t_1 increments) was carried out at 302 K, using a clean-MLEV17 pulse sequence (Griesinger et al., 1988) of 40 ms for the spin-lock period. A NOESY spectrum in H_2O was measured at 292 K with a mixing time of 180 ms, 80 scans, a spectral width of 23 809 Hz in both directions, 4K data points in the t_2 domain, and 800 t_1 increments. In order to conserve the magnetization of the exchangeable protons, the H_2O signal was suppressed by using a time-shared long pulse with the excitation minimum on the H_2O frequency as observation pulse (Haasnoot & Hilbers, 1983). By setting the carrier frequency exactly one-fourth of the total spectral width downfield from the H_2O frequency, the solvent signal could be further reduced by data-shift accumulation prior to the Fourier transform. The acquisition of 121-MHz ^{31}P NMR data was carried out on a Bruker AM300 spectrometer interfaced with an Aspect 2000 computer, using Bruker-DISNMR87 software. Broad-band ^{1}H-decoupled ^{31}P NMR spectra were recorded with two-level MLEV decoupling, using a Bruker 5-mm ^{1}H{^{31}P} probe. A total of 20 000 transients were collected with 1024 data points and a spectral width of 1502 Hz.

RESULTS AND DISCUSSION

One-Dimensional ^{1}H NMR Spectra in D_2O. Figure 1 shows the thymine methyl-proton region of the one-dimensional ^{1}H NMR spectrum of J4 in D_2O (5 mM $MgCl_2$; 50 mM NaCl) at two different temperatures. The addition of metal ions to the sample was suggested by studies of Duckett et al. (1988, 1990), which pointed out that complete folding of four-way junctions requires the presence of divalent cations. At the chosen conditions a single set of relatively sharp resonance lines is observed which implies that the DNA fragment J4 adopts a stable conformation. In the methyl-proton region, for example, a single set of 11 methyl-proton resonances appears. Except for one signal at 1.69 ppm which originates from T8, the thymine residue at the four-way branch point (vide infra), all methyl protons resonate outside the chemical-shift region common to methyl protons of thymine residues in a single-stranded stack or random-coil conformation (Altona, 1990). The methyl protons of three thymine residues resonate at a considerably lower field: ca. 2.00 ppm, the characteristic chemical-shift value for the first thymine residue in TT-minihairpin loops (Pieters et al., 1990; Blommers et al., 1991; Ippel et al., 1992). The other methyl protons resonate at a higher field as compared to the random coil: between 1.57 and 1.29 ppm. Methyl-proton signals of thymine residues in B-DNA type duplexes are commonly found in this spectral region (Van de Ven & Hilbers, 1988a; Altona, 1990), and also the methyl-proton signals of the second thymine residue in TT-minihairpin loops resonate in this region: ca. 1.32 ppm. Results of further experiments show (vide infra) that this conformation is in fact the four-way junction in which we are interested.

On raising the temperature, the resonance frequencies of the signals of J4 were found to shift gradually toward the frequencies expected for a random-coil conformation (data not shown). At temperatures below 290 K all signals show significant line broadening. This broadening was found to be less pronounced if the concentration of J4 was decreased. The effect is ascribed to self-association phenomena. The optimum combination of narrow resonance lines on the one hand, and a minimal shift of the methyl-proton signals toward the random-coil position on the other hand, was found at a temperature of ca. 302 K. For this reason most of the 2D NMR spectra were recorded at 302 K.

^{1}H NMR Spectra in H_2O. Figure 2 shows the imino-proton region of the one-dimensional ^{1}H NMR spectrum in H_2O and a part of the 180-ms NOESY spectrum in H_2O; the imino-proton region on the horizontal (ω_2) axis and the adenine-H2 and cytosine-C4NH$_2$ region on the vertical (ω_1) axis. Five imino-proton resonances are visible at low field between 13.5 and 14.2 ppm. This region is characteristic for the resonances of thymine-N3H imino protons in Watson–Crick type base pairs. The five intense cross peaks in the NOESY spectrum, representing the short distance between thymine-N3H and adenine-H2 typical for Watson–Crick type A·T base pairs, provide additional evidence for the presence of five intact A·T base pairs. The observation of five A·T base pairs, in combination with the evidence from the one-dimensional spectra in D_2O for the presence of three hairpin loops in J4, confirms that DNA fragment J4 is folded into a stable cruciform conformation. Moreover, even without sequential assignment of any of the exchangeable protons, we can conclude that at least two of the four junctional base pairs are intact. This conclusion is in accordance with the findings of Wemmer et al. (1985) that base pairing occurs at the site of branching. Unfortunately, we are unable to determine in a similar way the number of intact G·C base pairs in J4, due to overlapping guanine-N1H imino-proton signals.

Resonance Assignment of the Nonexchangeable Protons: General Considerations. In accordance with standard meth-

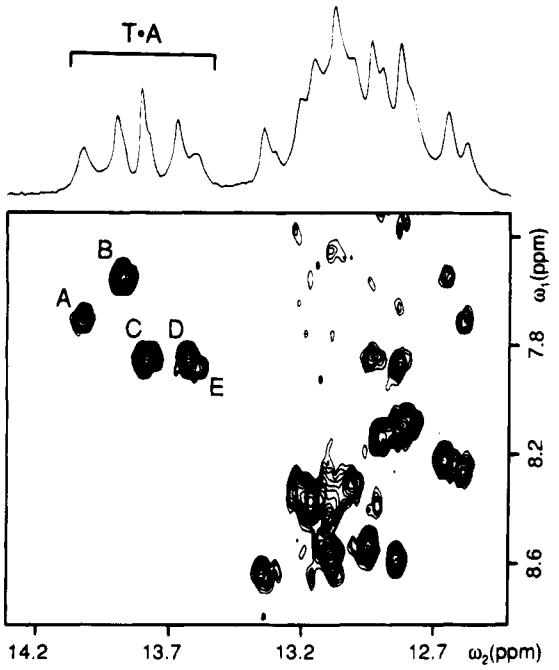

FIGURE 2: Imino-proton region of the one-dimensional ^1H NMR spectrum in H_2O and part of the 180-ms NOESY spectrum in H_2O (5 mM $MgCl_2$; 50 mM NaCl). The horizontal (ω_2) axis covers the spectral region common to the resonances of the thymine-N3H imino protons (13.5−14.2 ppm) and the guanine-N1H imino protons (12.5−13.5 ppm) in a Watson−Crick type base pair. The vertical (ω_1) axis covers the spectral region of the adenine-H2 (7.4−8.0 ppm) and the hydrogen-bonded cytosine-C4NH_2 resonances (8.0−8.8 ppm). The five cross peaks indicated with A−E correspond to short interstrand N3H(T)−H2(A) distances common to Watson−Crick type A•T base pairs.

ods as reviewed by Wüthrich (1986), the ^1H-resonance assignment proceeded in two stages. First, the spin systems of the cytosine and thymine bases and of the sugar-ring protons were identified. The HOHAHA experiment was satisfactory for finding most of these spin systems. However, no H6-Me cross peaks were observed, because the H6-Me coupling constants are smaller than the line widths. Therefore the H6-Me spin systems were identified in the 75-ms NOESY spectrum. In the second stage, the identified spin systems were assigned to specific residues in the DNA sequence using sequential cross peaks in the NOESY spectra. Usually the sequential NOE pattern is strongly dependent on the conformation of the oligonucleotide; therefore, sequential assignment and qualitative conformational analysis are closely interrelated. In the course of the interpretation of the NOESY spectra, J4 was found to contain three different structural motifs which had to be assigned with different strategies. (1) The three 5′-CTTG-3′ motifs show cross-peak patterns corresponding to H2-type minihairpin-loop structures. (2) The four arms of the four-way junction, constituting the major part of the oligonucleotide, show cross-peak patterns corresponding to a common B-DNA type double helix. (3) Conformational effects exclusively ascribed to the four-way junction are mainly observed in four residues in the center of the DNA sequence. The experimental data which were important for the assignment and the conformational analysis of each of these three motifs will be discussed in detail in separate subsections.

Anticipating the experimental data, the result of the ^1H-resonance assignment is given in Table 1. All H6, H8, H5, and methyl-proton resonances could be assigned, as well as

Table 1: Chemical-Shift Values of the Assigned Nonexchangeable Proton Resonances of the DNA Four-Way Junction J4[a]

residue	H6/H8	H2/H5/Me	H1′	H2′	H2″	H3′
G1	7.95		5.98	2.61	2.78	4.85
C2	7.47	5.46	5.67	2.12	2.45	4.88
A3	8.31	7.77	6.27	2.79	2.92	5.05
C4	7.30	5.25	5.82	1.95	2.46	4.70
T5	7.29	1.57	5.79	2.08	2.47	4.88
G6	7.89		5.90	2.65	2.72	5.01
C7	7.46	5.34	5.98	2.04	2.45	4.88
T8	7.71	1.69	6.32	2.35	2.89	4.91
A9	7.82	7.64	6.09	2.62	2.78	4.99
C10	7.35	5.22	5.67	1.93	2.32	?
G11	7.83		5.83	2.47	2.66	4.92
C12	7.49	5.42	6.18	2.04	2.27	?
T13	7.91	2.03	6.40	1.92	2.80	4.79
T14	7.56	1.34	5.45	1.78	2.07	4.62
G15	7.96		6.14	2.78	3.04	4.84
C16	7.37	5.37	5.81	2.14	2.51	4.77
G17	7.90		6.18	2.69	2.91	4.95
T18	7.30	1.45	6.02	2.17	2.59	4.88
C19	7.37	5.52	5.79	1.75	2.25	4.85
G20	7.87		5.74	2.78	2.76	5.00
G21	7.65		5.81	2.44	2.67	4.90
C22	7.44	5.38	6.13	2.01	2.26	?
T23	7.85	2.01	6.35	1.92	2.27	4.77
T24	7.56	1.33	5.45	1.78	2.07	4.60
G25	7.96		6.12	2.77	3.01	4.84
C26	7.44	5.35	6.13	2.09	2.54	4.80
C27	7.43	5.59	5.87	1.94	2.37	4.94
G28	8.10		6.16	2.56	3.20	4.94
C29	7.89	5.84	5.82	2.24	2.60	?
C30	7.59	5.70	5.53	1.98	2.32	4.82
A31	8.22	?	6.10	2.59	2.80	4.99
C32	7.44	5.41	6.01	1.99	2.24	?
T33	7.83	2.00	6.30	1.91	2.21	4.79
T34	7.49	1.30	5.45	1.76	2.05	4.58
G35	8.00		6.06	2.81	3.04	4.84
T36	7.24	1.43	5.96	2.01	2.51	4.85
G37	7.88		5.89	2.68	2.85	5.01
G38	7.58		5.64	2.49	2.72	4.96
A39	7.97	?	6.02	2.52	2.84	5.03
G40	7.70		5.68	2.51	2.62	4.97
C41	7.25	5.29	5.55	1.89	2.33	4.79
A42	8.17	?	6.03	2.73	2.88	5.02
G43	7.55		5.83	2.42	2.69	4.88
T44	7.11	1.29	5.83	1.97	2.40	4.85
G45	7.88		5.95	2.61	2.72	4.97
C46	7.49	5.49	6.21	2.16	2.20	4.49

[a] The values (relative to DSS, estimated accuracy <0.01 ppm) were extracted from the 350-ms 600-MHz NOESY spectrum (recorded in D_2O at 302 K) with a digital resolution of 2.7 Hz per point. Unsolved or ambiguous assignments are indicated with a question mark.

all resonances of the H1′, H2′, and H2″ sugar protons and the majority of the H3′ resonances. Attempts to assign the adenine-H2 resonances were successful for only two out of five H2 protons. This is probably due to overlap in combination with the usually small number of NOE connectivities to other protons. Stereospecific assignments of the H2′ and H2″ resonances were performed on the basis of the difference in intensity between the H1′−H2′ and H1′−H2″ cross peaks in the 75-ms NOESY spectrum. The most intense NOE was attributed to H2″. In cases where this method failed, mostly due to spectral overlap, the resonance at higher field was assigned to H2′. The latter assignment method, however, is not fully reliable, especially not for purine residues (Rinkel et al., 1986).

HOHAHA Spectrum in D_2O: Identification of the H5−H6 Spin Systems. The identification of the H5−H6 spin systems is shown in Figure 3. As is indicated in this figure,

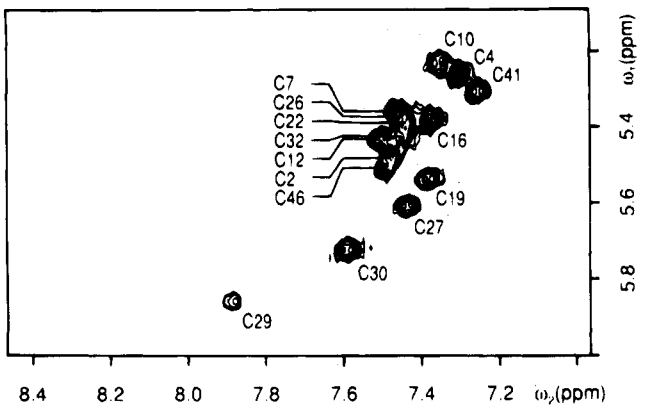

FIGURE 3: Part of the contour plot of the 600-MHz HOHAHA spectrum (recorded in D_2O at 302 K) showing the H5−H6 cross peaks. For each cross peak the assignment of the associated cytosine residue is specified. The small number of contour lines for the H5−H6 cross peak of C29, one of the residues directly adjacent to the branch point, is caused by line broadening.

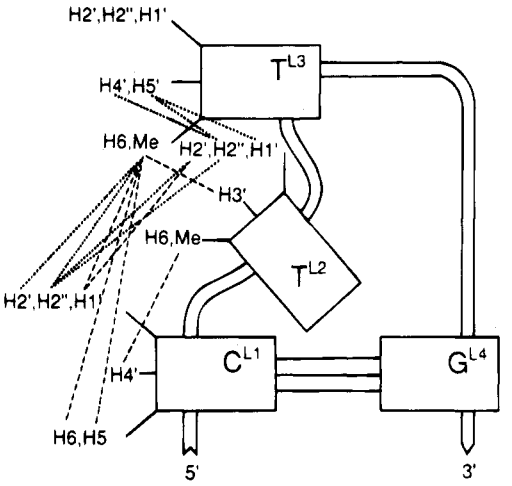

FIGURE 4: Schematic illustration of the conformation of the H2-type minihairpin loop. Dashed lines as well as dotted lines between protons represent unusual NOE contacts typical for an H2-type minihairpin loop, as emerged from previous studies of relatively small DNA fragments. Intraresidual NOE contacts, and NOEs similar to those observed in a standard B-DNA type conformation, are omitted in this representation. The dashed lines indicate the subset of typical NOE contacts which were observed unambiguously for all three 5′-CTTG-3′ motifs in the NOESY spectrum of J4. The remaining typical NOEs, represented with dotted lines, could not be ascertained for J4 due to spectral overlap.

all H5−H6 cross peaks of the 15 cytosine residues present in J4 can be observed separately in the HOHAHA spectrum. These data are shown here for several reasons. First, the remarkably good resolution of the H5−H6 cross peaks was an important factor in the assignment procedure. Secondly, the presence of a single, complete set of H5−H6 resonances is a strong indication that the molecule adopts a well-defined conformation. Finally, these data clearly show the presence of the H5−H6 cross peak of residue C29, which is one of the four residues in the center of the four-way junction. The relatively low intensity of this cross peak is caused by line-broadening, which phenomenon is observed for most of the protons of the four central residues.

The 5′-CTTG-3′ Minihairpin-Loop Motifs: Assignment and Conformational Aspects. Earlier, relatively small DNA fragments containing hairpin-loop structures with the sequential motif 5′-CTTG-3′ were studied thoroughly (Ippel et al., 1992; J. A. Pikkemaat and C. Altona, unpublished results). The TT-hairpin loops observed in these fragments show many conformational similarities with the 5′-CTAG-3′ containing TA-hairpin loop studied by Pieters et al. (1990) and with several other hairpin-loop structures observed in small DNA fragments containing the general motif 5′-$C^{L1}Y^{L2}X^{L3}G^{L4}$-3′ (Y = thymine or cytosine; X = thymine, cytosine, adenine, or guanine) (Ippel, 1994). All these hairpin-loop structures have in common that residue C^{L1} and residue G^{L4} form a normal Watson−Crick type base pair. The loop itself consists of two residues. A characteristic feature of this type of hairpin loop, which was designated H2-type minihairpin loop, is that residue L3 is stacked upon residue L1, whereas the residue between them, L2, is folded into the minor groove, as is schematically shown in Figure 4. These conformational properties, later also observed in a 5′-TTTA-3′ containing hairpin loop by Blommers et al. (1991), are reflected in the NMR spectra by a number of highly characteristic features (Pieters et al., 1990; Blommers et al., 1991; Ippel et al., 1992). The five most distinct NMR features common to all H2-type minihairpin loops studied thus far are (1) characteristic ^{31}P chemical shifts for residue L2 (low field) and L3 (high field), (2) characteristic ^1H chemical shifts (low field) for the H6, H5, Me, and H1′ protons of residue L2, (3) a γ^t torsion angle for residue L4 instead of the γ^+ torsion angle common to a B-DNA type duplex conformation, (4) complete absence of B-DNA type sequential NOEs between residues L3 and L4, and (5) a large number of unusual NOEs which are indicated in Figure 4. In the remainder of this subsection it will be shown on the basis of experimental evidence for these five characteristic features that three H2-type minihairpin loops are present in J4.

(1) Figure 5 displays the proton-decoupled ^{31}P NMR spectrum of J4 at 302 K. The assignment of the phosphorus signals is still unsolved. Nevertheless, important information concerning the conformation of the hairpin-loop regions is obtained from the ^{31}P NMR spectrum. We made use of the analogy with the previously studied dumbbell-shaped DNA fragment DB16 shown in Scheme 1. This compound contains two minihairpin loops with base sequences which exactly match the hairpin-loop sequences in arms B and D of J4. The phosphorus resonances of DB16 were completely assigned by means of a two-dimensional $^{31}P-^1H$ correlated NMR spectrum (J. A. Pikkemaat and C. Altona, unpublished results). DB16 shows two ^{31}P resonances at exceptionally low field, which originates from the ^{31}P atoms of T4 and T12, i.e., the residues T^{L2} in the minihairpin-loop motif which are folded into the minor groove, and two ^{31}P resonances at exceptionally high field, which belong to residues T5 and T13, i.e., the residues T^{L3} in the minihairpin-loop motif. The ^{31}P NMR spectrum of J4 shows three separate phosphorus signals at low field and three signals at high field with similar frequencies as found in the loop residues of DB16. These observations strongly indicate the presence of three H2-type minihairpin loops in J4.

(2) Three thymine residues, T13, T23, and T33, are readily recognized as residues L2 in the H2-type minihairpin-loop structure, because the chemical-shift values of the H6, Me, and H1′ protons (see Table 1) correspond with the characteristic (low field) values previously observed for residues L2 in 5′-$C^{L1}T^{L2}X^{L3}G^{L4}$-3′ containing minihairpin-loop struc-

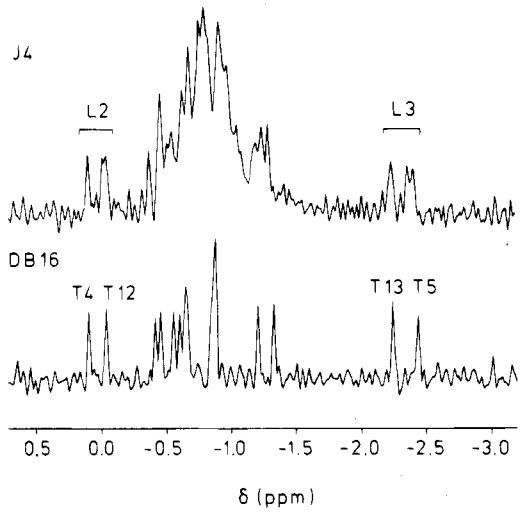

FIGURE 5: 121-MHz ^{31}P NMR spectrum of J4 at 302 K of the DNA four-way junction J4 and the dumbbell-shaped double-hairpin structure DB16. Although the phosphorus spectrum of J4 has not been assigned, chemical-shift analogy with ^{31}P NMR spectra of previously studied hairpin-loop structures in smaller DNA fragments indicates the presence of three H2-type minihairpin loops in the structure of J4. The assignments of the ^{31}P resonances belonging to residues L2 and L3 in the 5′-$C^{L1}T^{L2}T^{L3}G^{L4}$-3′ hairpin-loop motif of the completely assigned fragment DB16 is shown. As is highly characteristic for H2-type minihairpin loops, the phosphorus signals of residues L2 resonate at low field (ca. 0.0 ppm) and the phosphorus signals of residues L3 appear at high field (ca. −2.4 ppm). The other ^{31}P nuclei resonate in a relatively narrow region between −0.4 and −1.4 ppm.

tures (Pieters et al., 1990; Blommers et al., 1991; Ippel, 1994).

(3) The presence of γ^t torsion angles in residues G15, G25, and G35 could not be ascertained directly, due to unresolved J couplings. For each of these guanine residues, however, the NOESY spectrum shows an intense cross peak between the H8 proton and either the H5′ or the H5″ proton (data not shown). Although stereospecific assignment of the H5′ and the H5″ protons is not possible, this observation excludes the possibility of normal γ^+ torsion angles for residues G15, G25, and G35.

(4) The B-DNA type interresidual NOEs H1′/H2′/H2″-(n)−H8(n+1) are completely absent for the sequential pairs T14−G15, T24−G25, and T34−G35, even at a mixing time of 350 ms.

(5) A large number of typical NOEs for the H2-type minihairpin loop have been listed by Pieters et al. (1990) and Ippel (1994). As is shown in Figure 4, many of these typical NOEs were established with certainty for all three 5′-CTTG-3′ motifs in the base sequence of J4. For example, the highly characteristic long-range NOE H1′(C^{L1})−Me(T^{L3}) is well resolved for each hairpin loop (indicated in Figure 8).

The Duplex Domains in J4: Modified Strategy for the Sequential Assignment. Sequential ^{1}H NMR assignment of small (i.e., less than 15 base pairs) right-handed DNA duplexes has become a standard procedure during the last decade (Van de Ven & Hilbers, 1988b; Altona, 1990). This standard procedure makes use of the fact that the distances between the sugar H1′, H2′, and H2″ protons of an arbitrary residue, n, and the base protons H6/H8 of residue n as well as residue n+1 are sufficiently short (i.e., less than 5 Å) that NOE effects can be observed between the resonances of these protons. If the majority of these NOEs is well resolved in the NOESY spectrum, it is possible to use a straightforward assignment procedure. Starting with the proton resonances of a specific residue in the base sequence (not necessarily the first residue), protons of the other residues can be assigned by walking via a path of sequential NOEs successively through the entire strand. For a full account of this standard assignment method, see Wüthrich (1986). In case of spectral overlap, however, there are often several alternative assignments possible, which usually cannot be evaluated directly. In such a situation one has to carry out the assignment by means of an elimination procedure: for each alternative the sequential-assignment procedure has to be pursued until a contradiction is encountered with respect to the a priori known base sequence. Unambiguous assignment is accomplished if all but one of these alternatives can be proven contradictory. For long DNA fragments like J4, spectral overlap frequently occurs. In the NOESY spectrum presented here, ca. 60% of the H6/H8 base protons cannot be assigned directly, due to overlap. The list of alternative assignments which have to be administrated and evaluated one by one during the elimination process tends to become excessively large. As a consequence, the standard assignment procedure is extremely time-consuming for large DNA fragments and readily leads to ambiguous results. For this reason a modified sequential-assignment strategy was used, which is partly similar to the strategy used by Chen et al. (1991) for the assignment of two 64-mer four-way junctions. The modified strategy, in which the H5/Me protons are systematically taken into account, permits an efficient administration of temporarily incomplete results and therefore considerably facilitates the sequential assignment of large DNA fragments like J4.

The modified sequential-assignment strategy consists of two separate stages. In the first stage all sequential subfragments of the type 5′-RY-3′ and 5′-RYY-3′ (R purine and Y pyrimidine) are traced in the NOESY spectrum. For two reasons these specific subfragments can be found with considerably higher certainty and less effort than subfragments of the type 5′-RR-3′ and 5′-YR-3′. Except for the three "universal" sequential NOEs: H1′(n)−H6/H8(n+1), H2′(n)−H6/H8(n+1), and H2″(n)−H6/H8(n+1) that are found in a right-handed DNA duplex regardless of the type of the bases which are involved, four additional sequential NOEs are observed in cases where residue n+1 contains a pyrimidine base: H6/H8(n)−H5/Me(n+1), H1′(n)−H5/Me-(n+1), H2′(n)−H5/Me(n+1), and H2″(n)−H5/Me(n+1). The second reason is the usually better resolution of the H5 and Me signals as compared to the signals of H6 and H8.

In the second stage these subfragments are assigned to specific domains in the a priori known DNA sequence. This absolute assignment can be achieved by extending the sequential assignment of a subfragment in the 3′ and 5′ direction, until it uniquely matches a certain part of the DNA sequence. In some cases characteristic residues can be used as an anchor point for the absolute assignment, e.g., the first residue in the DNA sequence or the guanine residue in the 5′-CTTG-3′ minihairpin-loop motif, which can be identified in the NOESY spectrum by the characteristic ^{1}H chemical shifts and the absence of sequential NOEs with the proton resonances of the preceding residue. Spectral overlap can prohibit the subfragments to be extended directly to such a length that a unique match with the DNA sequence emerges.

Scheme 2. Observed Sequential and Long-Range NOEs in J4, As Derived from the 350-ms 600-MHz NOESY Spectrum (Recorded in D_2O at 302 K)[a]

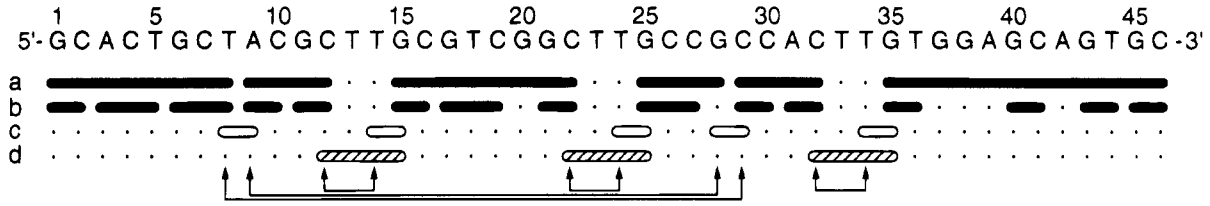

[a] The black bars on line a indicate the presence of the B-DNA type NOEs, H1′(n)−H6/H8(n+1), H2′(n)−H6/H8(n+1), and H2″(n)−H6/H8(n+1). The black bars on line b indicate the presence of the additional B-DNA type NOEs in case n+1 is a pyrimidine residue, H6/H8(n)−H5/Me(n+1), H1′(n)−H5/Me(n+1), H2′(n)−H5/Me(n+1), and H2″(n)−H5/Me(n+1). Complete absence of sequential NOEs between two consecutive residues is specified with a white bar on line c. The parts in the sequence showing the typical NOE pattern for H2-type minihairpin loops are indicated with hatched bars on line d. Long-range NOEs are indicated with arrows pointing at the residues concerned.

In these cases the assignment has still to be performed by elimination. But as small subfragments instead of single residues are used in the elimination process, the number of possibilities that have to be checked is limited.

In the case of fragment J4, the well-defined sequential subfragments 5′-RY-3′ and 5′-RYY-3′ that must be searched for in the first stage of the new assignment strategy were characterized relatively easily in the NOESY spectrum. The experimentally collected subfragments are shown in Scheme 2. In the second stage the absolute assignment of these subfragments with respect to the base sequence was accomplished. For subfragments 5′-$A^3C^4T^5$-3′, 5′-$G^6C^7T^8$-3′, and 5′-$G^{17}T^{18}C^{19}$-3′ the absolute assignment was almost trivial on account of their unique occurrence in the base sequence of J4. Although 5′-$G^{15}C^{16}$-3′, 5′-$G^{25}C^{26}C^{27}$-3′, and 5′-$G^{35}T^{36}$-3′ occur more than once, the absolute assignment of these subfragments was also straightforward because residues G15, G25, and G35 were directly identified as guanine residues of the 5′-CTTG-3′ minihairpin-loop motif on account of the characteristic H2″ chemical shift and the absence of interresidual NOEs, H1′/H2′/H2″(T^{L3})−H8(G^{L4}). The characteristic NMR pattern of the first residue of each minihairpin-loop motif, C12, C22, and C32, was helpful regarding the absolute assignment of subfragments 5′-$G^{11}C^{12}$-3′, 5′-$G^{21}C^{22}$-3′, and 5′-$A^{31}C^{32}$-3′. However, as these subfragments cannot be distinguished from each other on the basis of the spin patterns of the base protons, the sequential assignment of at least two of these subfragments had to be extended toward the residue at the 5′ end. For one subfragment the extra residue at the 5′ end was found to be a purine residue, and for the other two subfragments the extra residues were cytosine residues which, in turn, were parts of other subfragments, 5′-RC-3′ and 5′-CC-3′. The resulting extended subfragments can now be distinguished from each other and, as a consequence, the absolute assignment of the extended subfragment 5′-$G^{20}G^{21}C^{22}$-3′ and of the combined subfragments, 5′-$A^9C^{10}G^{11}C^{12}$-3′ and 5′-$C^{29}C^{30}A^{31}C^{32}$-3′, is completed. The remaining residues could be assigned in a similar way by carefully extending the previously assigned fragments.

The Duplex Domains in J4: Description of the Sequential NOEs. The parts in the sequence of J4 showing the sequential-NOE path via the H1′, H2′, and H2″ in the 350-ms NOESY spectrum are indicated in Scheme 2. The presence of the sequential NOE path suggests that the arms adopt a right-handed helical conformation. Additional information from the NMR spectra strongly indicates a regular B-DNA conformation for these parts of the molecule. (1) All glycosidic torsion angles, χ, are in the *anti* conformation, as gauged from the relatively low intensity of the intraresidual H1′−H6/H8 cross peaks in the 75-ms NOESY spectrum and the markedly strong intraresidual H2″−H6/H8 NOEs. (2) The large line widths of the proton resonances preclude a proper determination of the N/S ratio of the sugar moieties on the basis of J-coupling constants. However, the N/S ratio can be roughly monitored via the intensity of the intraresidual H3′−H6/H8 NOE. For a combination of χ-*anti* and a high percentage N-type conformation, this cross peak is expected to be very intense. Except for the terminal residues G1 and C46 which show fraying effects, no such intense H3′−H6/H8 NOEs are observed. (3) The relative intensities of the individual cross peaks involved in the sequential-NOE path via the H1′, H2′, and H2″ protons differ substantially for either type of right-handed helix, A-DNA or B-DNA, provided the mixing time is sufficiently short (Wüthrich, 1986). For the residues in the duplex domains of J4, B-DNA type cross-peak intensities are observed in the 75-ms NOESY spectrum, i.e., H2′(n−1)−H6/H8(n) < H2″(n)−H6/H8(n) < H2″(n−1)−H6/H8(n) < H2′(n)−H6/H8(n) instead of A-DNA type intensities: H2″(n)−H6/H8(n) < H2′(n)−H6/H8(n) < H2″(n−1)−H6/H8(n) < H2′(n−1)−H6/H8(n).

As an example, the sequential-NOE path between the base protons H6/H8 and the sugar H1′ protons is shown in Figure 6. Similar NOEs were observed between H6/H8 and H2″ and between H6/H8 and H2′ (not shown). The sequential-NOE path is intact from the first residue in the sequence, G1, up to residue T8. No sequential NOEs were observed between residues T8 and A9. Instead, long-range NOEs were found between T8 and C29. At this point in the sequence the conformation of the molecule has to differ substantially from standard B-DNA. Then again we found B-DNA type sequential NOEs from C29 to residue C32, the beginning of the hairpin-loop motif. The residues C32, T33, T34, and G35 show the characteristic NMR patterns of an H2-type minihairpin loop. The sequential-NOE path starts again at residue G35 and continues up to the final residue C46 without interruptions. Now the sequential-NOE path through the duplex parts of arm A and arm D is complete. In a similar way we could identify the sequential-NOE paths in the remaining two arms of the four-way junction. Residues C12, T13, T14, and G15 of arm B and residues C22, T23, T24, and G25 of arm C show NMR patterns which are highly similar to the pattern of the sequence C32, T33, T34, and G35 in arm D, which we attribute to the presence of H2-type minihairpin-loop conformations in these parts of the molecule. The other residues in arm B and arm C all show normal B-DNA type sequential NOEs, except for the

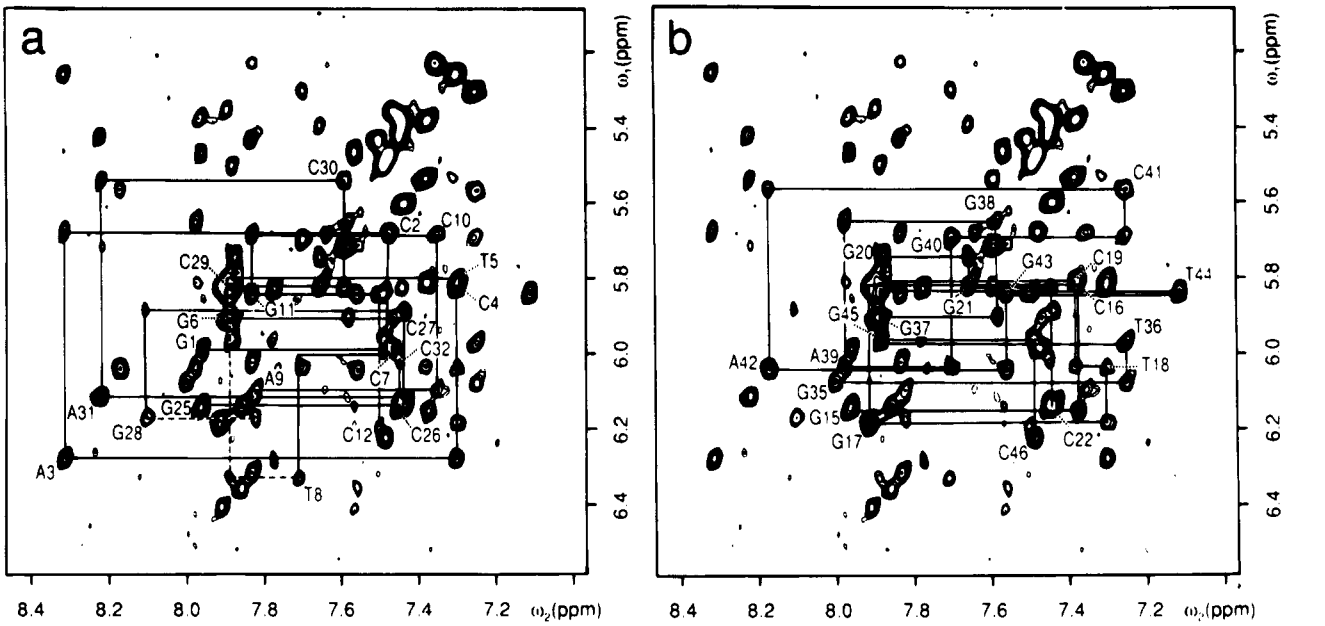

FIGURE 6: Part of the 350-ms 600-MHz NOESY spectrum (recorded in D_2O at 302 K) showing the sequential-NOE path via H1′(*n*)–H6/H8(*n*) and H1′(*n*)–H6/H8(*n*+1) cross peaks in the B-DNA type duplex domains of J4. (a) Illustration of the sequential-NOE paths going from residue G1 to T8, from C29 to C32, from G25 to G28, and from A9 to C12. The dashed lines indicate long-range NOE contacts between H1′(T8) and H6(C29) and between H1′(G28) and H8(A9). (b) Illustration of the sequential-NOE paths going from residue G15 to C22 and from residue G35 to C46.

two central residues A9 and G28. Instead of B-DNA type NOEs, H1′/H2′/H2″(T8)–H8(A9) and H1′/H2′/H2″(G28)–H6(C29), we found long-range NOEs H1′/H2′/H2″(G28)–H8(A9) between these residues, which is another indication that the conformation at the center of the four-way junction deviates severely from standard B-DNA.

The Conformation at the Center of the Four-Way Junction. Altogether, the experimental evidence for the presence of hairpin-loop structures at the three 5′-CTTG-3′ motifs, B-DNA type conformations for all four arms of the junction (except for residues at the center), and the presence of all five A•T base pairs strongly suggest that J4 does contain a four-way junction. In this subsection, the conformation at the center of the junction will be discussed. Biochemical experiments by Cooper and Hagerman (1987) and Duckett et al. (1988) have shown that in the presence of Mg^{2+} the four arms of Holliday junctions lack the symmetry necessary for a planar or tetrahedral conformation. Instead of pointing each to a different direction, the four arms are rotated in such a way that they form two quasicontinuous, fully stacked double helices (Figure 7). In fact, the planar or tetrahedral conformation can be considered as the central intermediate between two different fully stacked conformations, J4-I and J4-II, which are sometimes called cross-over structures. As is suggested by the schematic illustration in Figure 7, the differences between the three hypothetical conformations are mainly determined by the differences in the sequential base–base stacking patterns of eight residues in the center of the junction: T8, A9, T18, C19, G28, C29, G38, and A39. In a planar or tetrahedral conformation, severe discontinuities in the usual sequential stacking are expected to occur between T8 and A9, T18 and C19, G28 and C29, and G38 and A39. For each of the eight central residues a base–base stacking interaction is missing, either at the 3′ or at the 5′ side of the residue. In a cross-over conformation, however, full base–base stacking is retained for all central residues. Four out of the eight central residues show continuous stacking

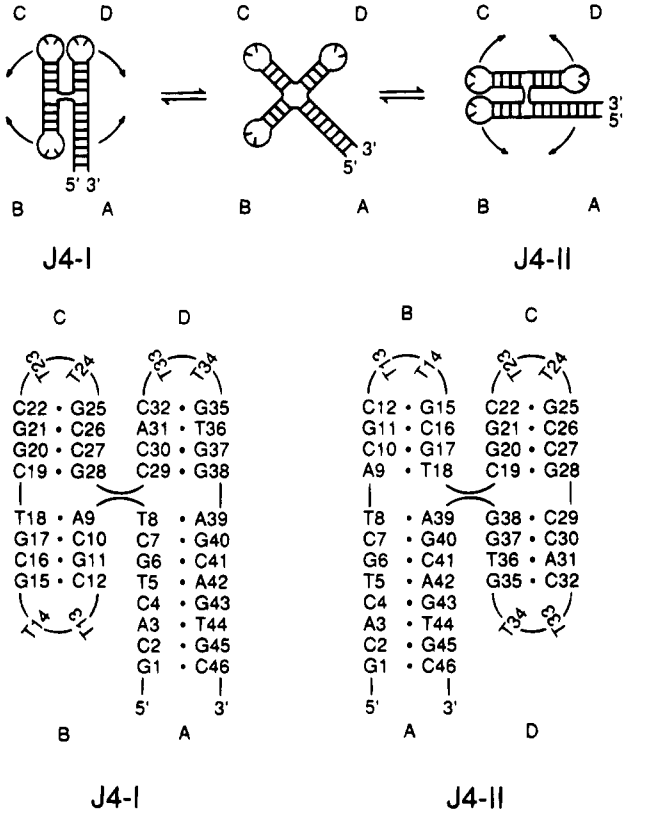

FIGURE 7: Schematic illustration of three hypothetical conformations in four-way junctions. The planar or tetrahedral conformation can be considered as the intermediate between two different, fully stacked conformations, J4-I and J4-II. The transition between these hypothetical conformations can be brought about by a rotation of the four arms of the junction relative to each other. The difference between J4-I and J4-II with respect to the arrangement of the stacked arms in the quasicontinuous helices is immediately clear from this illustration.

between sequentially adjacent residues. For the remaining four central residues, however, stacking between adjacent

residues is lost and replaced by unusual, quasicontinuous stacking between residues far apart in the DNA sequence. The latter set of four central residues comprises the branch point, i.e., the site of the junction at which two sugar–phosphate backbones cross from one quasicontinuous duplex to the other. For conformer J4-I, these residues are T8, A9, G28, and C29, whereas for the other fully stacked conformer J4-II these residues are T18, C19, G38, and A39.

Sequential base–base stacking can be probed efficiently with NMR methods. Exactly the same methods can be used to investigate base–base stacking between the central eight residues of J4. A first indication about the conformation of J4 is the observation that the proton resonances of residues T8, A9, G28, and C29 have markedly larger line widths than the other proton resonances and chemical-shift values that deviate substantially from the values found in a regular B-DNA type conformation (see Table 1). The other four central residues, T18, C19, G38, and A39, behave in a relatively normal fashion. This observation suggests that residues T8, A9, G28, and C29 are the residues directly adjacent to the branch point. This situation is exclusively met in conformation J4-I. Broadening of ^{1}H resonances of residues at the center of the four-way junction was also observed by Chen et al. (1991). The origin of this effect is not clear; a plausible explanation is the occurrence of local conformational changes.

More convincing evidence for the presence of conformation J4-I is supplied by interresidual NOEs observed between the eight central residues of the junction. For two residues, *m* and *n*, being stacked in a regular B-DNA fashion (residue *n* being stacked upon the 3′ side of residue *m*) we expect, depending on the type of residue *n*, the following interresidual cross peaks in a NOESY spectrum with sufficiently long mixing time: H1′(*m*)–H6/H8(*n*), H2′(*m*)–H6/H8(*n*), H2″(*m*)–H6/H8(*n*), H6/H8(*m*)–H5/Me(*n*), H1′(*m*)–H5/Me(*n*), H2′(*m*)–H5/Me(*n*), and H2″(*m*)–H5/Me(*n*) (Wüthrich, 1986). In the 350-ms NOESY spectrum of J4 we systematically checked for the eight central residues whether these cross peaks are present or not (Figure 8). The results are summarized in Table 2. Although not every NOE is actually informative due to overlap, the observed NOEs strongly indicate sequential stacking between residues T18 and C19 and between residues G38 and A39, and absence of sequential stacking between residues T8 and A9 and between residues G28 and C29. This corresponds with the situation in cross-over structure J4-I. Moreover, several unambiguous long-range NOEs are found between residues G28 and A9 and between residues T8 and C29, in spite of the relatively large line widths of the proton resonances involved. These data imply that arm A of the four-way junction is stacked more or less regularly upon arm D and arm B on arm C, as shown schematically in Figure 9. By contrast, none of the expected cross peaks for cross-over isomer J4-II (listed in Table 2) is present in the NOESY spectrum, except for a weak signal at the position where the NOE between H2″(G38) and H6(C19) is expected. This could be a spurious peak, or it may reflect the presence of a minor amount of conformation J4-II. However, if conformation J4-II is present, it has to be in fast exchange (relative to the NMR time scale) with conformation J4-I, as only a single set of resonances is observed in the NMR spectra. This seems to be rather unlikely on account of the large conformational changes which have to occur within the molecule during a transition of J4-I to J4-II. Apart from the NOEs given in Table 2, two additional experimentally observed long-range NOEs plead for conformation J4-I: H2(A9)–H1′(C19) and H8(A9)–H8(G28). These NOEs correspond in idealized models of B-DNA to distances slightly larger than 5 Å but are likely to appear at the relatively long mixing time used in this study.

CONCLUSIONS AND PERSPECTIVES

New high-resolution NMR data concerning the conformation of DNA four-way junctions in solution are presented and discussed. For these studies an immobilized Holliday junction was constructed consisting of 46 residues, i.e., 16 residues less than the immobilized four-way junctions used in NMR studies by Chen et al. (1991, 1993). Whereas the compounds used by Chen et al. are composed of four separate DNA strands, the present Holliday junction consists of a single, linear DNA oligomer. This is achieved through the presence of three minihairpin-loop motifs 5′-CTTG-3′ in the sequence, capping the ends of three branches of the junction. Thus, only one branch remains with an open-ended duplex stem. As the TT-hairpin loops prevent the duplex stems from dissociating, the number of base pairs in these capped stems can be restricted to four, which is substantially less than the eight base pairs normally used for a stable open-ended duplex stem. The relatively small size of the compound and the thorough knowledge of the characteristic 5′-CTTG-3′ minihairpin-loop motif, obtained from studies of smaller DNA fragments containing the same sequence, make this four-way junction a suitable model compound for detailed NMR studies.

From the reported NMR data of J4 (at a temperature of 302 K and in the presence of Mg^{2+}) a well-defined secondary structure emerges. This NMR secondary structure contains three H2-type minihairpin loops, formed by the three 5′-CTTG-3′ motifs in the DNA sequence. For the remaining part of the DNA fragment the observed NOE patterns indicate the presence of a regular B-DNA conformation, except for the eight residues at the center of the four-way junction, T8, A9, T18, C19, G28, C29, G38, and A39. Full base pairing occurs for all residues of J4, including the eight central residues, except for the six thymine residues in the hairpin loops. Unusual NOE connectivities between the eight central residues provide direct evidence for the presence of coaxial stacking between arms A and D and between arms B and C of the junction. This suggests a structure consisting of two quasicontinuous duplexes, connected to each other at the branch point through two short sugar–phosphate backbone parts crossing from one duplex to the other. No substantial evidence was found for the alternative, equally imaginable, cross-over structure in which coaxial stacking occurs between arms A and B and between arms C and D. The remarkably strong conformational preference for one cross-over conformer rather than the other is confirmed by previous observations of various other four-way junctions (Cooper & Hagerman, 1987; Duckett et al., 1988; Guo et al., 1991), and it is often assumed that this phenomenon governs the outcome of homologous recombination in the living cell. For this reason, it is tempting to unravel the underlying mechanism. One of the mechanisms that have been proposed to govern the conformational preference is the free energy of the base–base stacking interaction at the center of the four-way junction. This seems to be confirmed

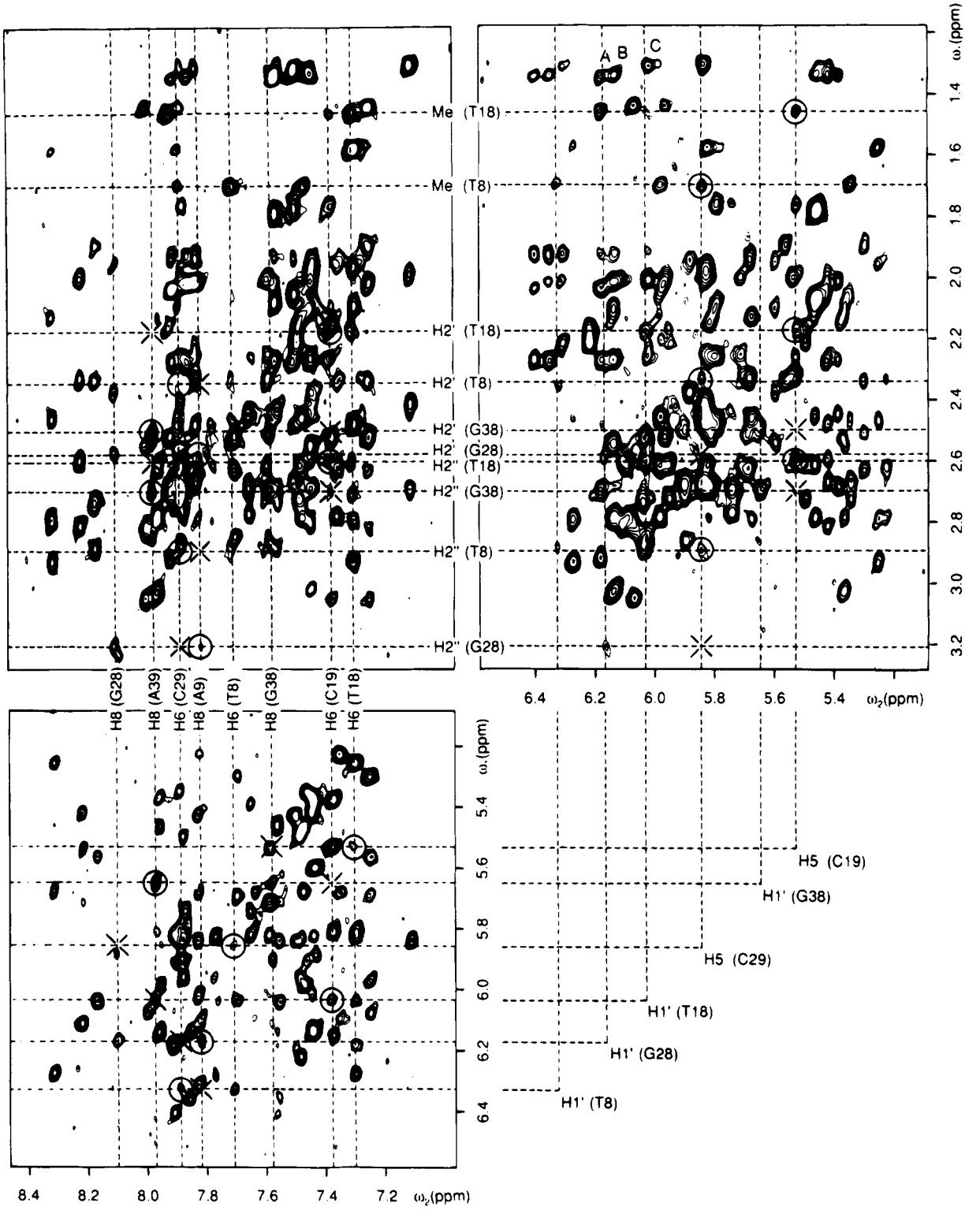

FIGURE 8: Three different parts of the 350-ms 600-MHz NOESY spectrum of J4 (recorded in D_2O at 302 K). The dashed lines represent the resonance positions of the protons in Table 2, which are decisive in the determination of the stacking pattern, J4-I or J4-II. The positions where NOEs should be present in case of a stacking pattern as in conformation J4-I are indicated with a circle (O), and the positions where NOEs should be present for the stacking pattern occurring in J4-II are indicated with a diagonal cross (×). One of the characteristic NOEs for an H2-type minihairpin loop, H1′(C^{L1})−Me(T^{L3}), is indicated for each 5′-$C^{L1}T^{L2}T^{L3}G^{L4}$-3′ motif in the sequence of J4. The cross peak marked with A corresponds to H1′(C12)−Me(T14), the cross peak marked with B to H1′(C22)−Me(T24), and C to H1′(C32)−Me(T34).

by the observation that the nature of the eight central residues influences the population of both cross-over conformers. However, Guo et al. (1991) showed that the conformational preference for several of the four-way junctions studied could not be explained strictly on the basis of the differences in the nearest-neighbor stacking interaction between the two alternative cross-over conformers. The molecule J4 has a base sequence which differs at the branch point from the previously studied four-way junctions. Using the values for the nearest-neighbor stacking energies of Delcourt and Blake (1991) at 75 mM Na^+ for J4, the calculated free energy (at 302 K) of the preferred cross-over conformation J4-I is in

Table 2: Systematic List of NOEs between Protons at the Branch Point of the Four-Way Junction As Predicted by Models J4-I and J4-II and the Experimental Evidence for These NOEs in the 350-ms 600-MHz NOESY Spectrum

NOEs predicted by model J4-I[a]	experimental evidence[b]	NOEs predicted by model J4-II[a]	experimental evidence[b]
H1′(T18)−H6(C19)	+	H1′(T8)−H8(A9)	−
H6(T18)−H5(C19)	+	H2′(T8)−H8(A9)	? overlap
H2′(T18)−H6(19)	? overlap	H2″(T8)−H8(A9)	−
H2″(T18)−H6(C19)	+	H1′(G28)−H6(C29)	? overlap
H2′(T18)−H5(C19)	+	H8(G28)−H5(C29)	−
H2″(T18)−H5(C19)	+	H2′(G28)−H6(C29)	? overlap
Me(T18)−H5(C19)	+	H2″(G28)−H6(C29)	−
H1′(G38)−H8(A39)	+	H2′(G28)−H5(C29)	−
H2′(G38)−H8(A39)	? overlap	H2″(G28)−H5(C29)	−
H2″(G38)−H8(A39)	+	H1′(T18)−H8(A39)	? overlap
H1′(G28)−H8(A9)	+	H2′(T18)−H8(A39)	−
H2′(G28)−H8(A9)	? overlap	H2″(T18)−H8(A39)	−
H2″(G28)−H8(A9)	? very weak	H1′(G38)−H6(C19)	−
H1′(T8)−H6(C29)	+	H8(G38)−H5(C19)	? overlap
H6(T8)−H5(C29)	+	H2′(G38)−H6(C19)	? overlap
H2′(T8)−H6(C29)	? very weak	H2′(G38)−H6(C19)	+
H2″(T8)−H6(C29)	? overlap	H2′(G38)−H5(C19)	−
H2′(T8)−H5(C29)	+	H2″(G38)−H5(C19)	? very weak
H2″(T8)−H5(C29)	+		
Me(T8)−H5(C29)	+		

[a] Systematic list of interresidual NOEs expected at the center of the four-way junction in case of cross-over structure J4-I (J4-II). B-DNA type stacking is assumed between the eight residues, T8, A9, T18, C19, G28, C29, G38, and A39. The theoretical NOE lists are based on the list of short sequential distances (smaller than ca. 5 Å) between nonexchangeable protons in a standard B-DNA conformation given by Wüthrich (1986). Short sequential distances involving H3′, H4′, H5′, and H5″ are left out of consideration. [b] Experimental evidence for the presence of cross peaks in the 350-ms 600-MHz NOESY spectrum at the positions associated with the theoretical NOEs predicted by model J4-I (J4-II). A plus sign symbolizes that the corresponding cross peak was established unambiguously in the NOESY spectrum; a minus sign denotes the complete absence of the cross peak; a question mark indicates either that no conclusion can be drawn due to spectral overlap in the NOESY spectrum at the position of the cross peak concerned or that the actual presence of the cross peak is uncertain as a result of the low intensity.

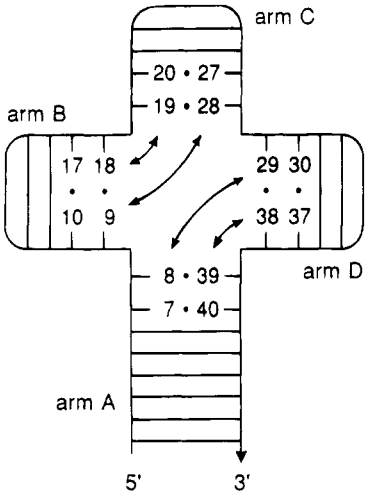

FIGURE 9: Schematic illustration of J4 summarizing the critical NOE contacts observed at the center of the four-way junction. These NOEs indicate that quasicontinuous stacking occurs at the interface between arms A and D and at the interface between arms B and C.

fact 1.3 kJ/mol higher than the free energy of the alternative cross-over conformation J4-II. This suggests that at least one other important factor is involved in the mechanism controlling the relative stabilities of the two cross-over conformers. We are tempted to speculate that the relative stability is strongly influenced by the ability of the cross-over structure to accommodate the two negatively charged phosphate groups of the exchanging strands at the branch point, i.e., the phosphate groups of residues A9 and C29 in cross-over conformer J4-I or residues C19 and A39 in cross-over conformer J4-II.

A second aspect which is of importance for the conformation of four-way junctions is the orientation of one quasi-continuously stacked double helix with respect to the other. This conformational aspect has been studied in the past with experimental techniques: fluorescence energy transfer on a set of junctions with pairs of donor and acceptor fluorophores attached to the arms, neutron scattering and electric birefringence, as well as molecular modeling. The results, reviewed by Duckett et al. (1992) and by Lilley and Clegg (1993), suggest that the helix axes of both quasicontinuous helices meet at an angle of ca. 60°. For conformer J4-I in Figure 7 this corresponds with a right-handed rotation of one helix with respect to the other about a virtual horizontal axis through the branch point over an angle of 60°. In spite of many efforts, no information about this specific conformational aspect could be obtained from the NMR spectra of J4. The nonexchangeable base protons and the sugar H1′, H2′, and H2″ protons were extensively searched for possible NOE contacts between two protons each belonging to a different quasicontinuous helix. Although, because of overlap, we cannot be completely certain that these interhelical NOE contacts are absent, no such NOEs were found. The apparent absence of these NOEs is in correspondence with molecular modeling studies (Von Kitzing et al., 1990; Macke et al., 1992), which predict short (less than ca. 5 Å) interhelical proton−proton distances only for protons in the vicinity of the branch point and attached to the sugar−phosphate backbone (H3′, H4′, H5′, and H5″). NOEs of these protons could not be interpreted unambiguously due to extensive overlap in this region of the NMR spectra of J4. According to these models, the end-to-end distances between the arms of the four-way junction J4 cannot be reliably determined by NMR, because the corresponding long-distance constraints (more than 10 Å) cannot be resolved. However, most data currently available suggest that the deviations from the B-DNA conformation are mainly confined to the site of strand exchange. If this is the case, the angle between both quasicontinuous helices will be strongly correlated with the main rotamers about the backbone bonds at the branch point. Torsion angles β, γ, and ϵ can in principle be studied via vicinal $J_{(HH)}$, $J_{(HP)}$, and $J_{(CP)}$ couplings. However, problems concerning the assignment of these protons and line-broadening effects prevent a proper determination of the coupling constants. NOE data, which are usually less sensitive to broad resonance lines, suggest γ^+ torsion angles for residues A9 and C29, as no strong NOEs of the H6/H8 proton to the H5′ or the H5″ proton were observed.

The next stage in the conformational studies of four-way junctions will be the collection of reliable distance constraints, especially at the cross-over point. First, however, several problems have to be solved. The necessary, improved spectral resolution, in particular of the resonances displayed by the H4′, H5′, and H5″ protons at the branch point, might be attainable with homonuclear 3D NMR methods, heteronuclear 3D NMR methods in combination

with site-specific isotopic enrichment, or by a further reduction of the size of the model compound. Currently, the structure determination of J4 is seriously handicapped by the broad resonances observed for the protons at the branch point, probably reflecting conformational averaging in the intermediate fast exchange regime. This may be solved by choosing different experimental conditions or changing the sequence of the model compound, though one could also argue that the conformational flexibility at the cross-over point might be an intrinsic, functionally significant, property of four-way junctions.

ACKNOWLEDGMENT

600-MHz NMR spectra were recorded at the Dutch National Hf-NMR facility (Nijmegen, The Netherlands) and at Bruker Inc. (Karlsruhe, Germany). We thank C. Erkelens (Leiden), J. J. M. Joordens (Nijmegen), and Dr. W. Bermel (Karlsruhe) for their assistance with the experiments.

REFERENCES

Altona, C. (1990) in *Landolt-Börnstein New Series VII/1c* (Saenger, W., Ed.) pp 88−190, Springer-Verlag, Berlin.

Bell, L. R., & Byers, B. (1979) *Proc. Natl. Acad. Sci. U.S.A. 76*, 3445−3449.

Blommers, M. J. J., Van de Ven, F. J. M., Van der Marel, G. A., Van Boom, J. H., & Hilbers, C. W. (1991) *Eur. J. Biochem. 201*, 33−51.

Chen, S.-M., Heffron, F., Leupin, W., & Chazin, W. J. (1991) *Biochemistry 30*, 766−771.

Chen, S.-M., Heffron, F., & Chazin, W. J. (1993) *Biochemistry 32*, 319−326.

Cooper, J. P., & Hagerman, P. J. (1987) *J. Mol. Biol. 198*, 711−719.

Delcourt, S. G., & Blake, R. D. (1991) *J. Biol. Chem. 266*, 15160−15169.

De Massey, B., Studier, F. W., Dorgai, L., Appelbaum, F., & Weisberg, R. A. (1984) *Cold Spring Harbor Symp. Quant. Biol. 49*, 715−726.

Duckett, D. R., Murchie, A. I. H., Diekmann, S., Von Kitzing, E., Kemper, B., & Lilley, D. M. J. (1988) *Cell 55*, 79−89.

Duckett, D. R., Murchie, A. I. H., & Lilley, D. M. J. (1990) *EMBO J. 9*, 583−590.

Duckett, D. R., Murchie, A. I. H., Bhattacharyya, A., Clegg, R. M., Diekmann, S., Von Kitzing, E., Kemper, B., & Lilley, D. M. J. (1992) *Eur. J. Biochem. 207*, 285−295.

Gellert, M., Mizuuchi, K., O'Dea, M. H., Ohmori, H., & Tomizawa, J. (1979) *Cold Spring Harbor Symp. Quant. Biol. 43*, 35−40.

Gierer, A. (1966) *Nature 212*, 1480−1481.

Griesinger, C., Otting, G., Wüthrich, K., & Ernst, R. R. (1988) *J. Am. Chem. Soc. 110*, 7870−7872.

Guo, Q., Lu, M., & Kallenbach, N. R. (1991) *Biopolymers 31*, 359−372.

Haasnoot, C. A. G., & Hilbers, C. W. (1983) *Biopolymers 22*, 1259−1266.

Hartel, A. J., Lankhorst, P. P. L., & Altona, C. (1982) *Eur. J. Biochem. 129*, 343−357.

Holliday, R. (1964) *Genet. Res. 5*, 282−304.

Hseih, T., & Wang, J. C. (1975) *Biochemistry 14*, 527−535.

Hsu, P. L., & Landy, A. (1984) *Nature 311*, 721−726.

Ippel, J. H., (1994) Thesis, Leiden, The Netherlands.

Ippel, J. H., Lanzotti, V., Galeone, A., Mayol, L., Van den Boogaart, J. E., Pikkemaat, J. A., & Altona, C. (1992) *J. Biomol. Struct. Dyn. 9*, 1−16.

Jeener, J., Meier, B. H., Bachmann, P., & Ernst, R. R. (1979) *J. Chem. Phys. 71*, 4546−4553.

Kallenbach, N. R., Ma, R.-I., & Seeman, N. C. (1983) *Nature 305*, 829−831.

Von Kitzing, E., Lilley, D. M. J., & Diekmann, S. (1990) *Nucleic Acids Res. 18*, 2671−2683.

Lilley, D. M. J. (1980) *Proc. Natl. Acad. Sci. U.S.A. 77*, 6468−6472.

Lilley, D. M. J., & Clegg, R. M. (1993) *Annu. Rev. Biophys. Biomol. Struct. 22*, 299−328.

Macke, T., Chen, S.-M., & Chazin, W. J. (1992) in *Structure & Function 1* (Sarma, R. H., & Sarma, M. H., Eds.) pp 213−227, Adenine Press, Schenectady, NY.

Macura, S., & Ernst, R. R. (1980) *J. Mol. Phys. 41*, 95−117.

Macura, S., Huang, Y., Suter, D., & Ernst, R. R. (1981) *J. Magn. Reson. 43*, 259−281.

Marion, D., & Wüthrich, K. (1983) *Biochem. Biophys. Res. Commun. 113*, 967−974.

Meselson, M. S., & Radding, C. H. (1975) *Proc. Natl. Acad. Sci. U.S.A. 72*, 358−361.

Mizuuchi, K., Kemper, B., Hays, J., & Weisberg, R. A. (1982) *Cell 29*, 357−365.

Orr-Weaver, T. C., Szostak, J. W., & Rothstein, R. J. (1981) *Proc. Natl. Acad. Sci. U.S.A. 78*, 6354−6358.

Panayotatos, N., & Wells, R. D. (1981) *Nature 289*, 466−470.

Pieters, J. M. L., De Vroom, E., Van der Marel, G. A., Van Boom, J. H., Koning, T. M. G., Kaptein, R., & Altona, C. (1990) *Biochemistry 29*, 788−799.

Platt, J. R. (1955) *Proc. Natl. Acad. Sci. U.S.A. 41*, 181−183.

Rinkel, L. J., Sanderson, M. R., Van der Marel, G. A., Van Boom, J. H., & Altona, C. (1986) *Eur. J. Biochem. 159*, 85−93.

Seeman, N. C. (1982) *J. Theor. Biol. 99*, 237−247.

Seeman, N. C., & Kallenbach, N. R. (1983) *Biophys. J. 44*, 201−209.

Symington, L., & Kolodner, R. (1985) *Proc. Natl. Acad. Sci. U.S.A. 82*, 7247−7251.

Thompson, B. J., Camien, M. N., & Warner, R. C. (1976) *Proc. Natl. Acad. Sci. U.S.A. 73*, 2299−2303.

Van de Ven, F. J. M., & Hilbers, C. W. (1988a) *Nucleic Acids Res. 16*, 5713−5726.

Van de Ven, F. J. M., & Hilbers, C. W. (1988b) *Eur. J. Biochem. 178*, 1−38.

Wemmer, D. E., Wand, A. J., Seeman, N. C., & Kallenbach, N. R. (1985) *Biochemistry 24*, 5745−5749.

Wüthrich, K. (1986) in *NMR of Proteins and Nucleic Acids*, John Wiley & Sons, New York.